

An optical recording system based on a fast CCD sensor for biological imaging

F. Mammano,¹ M. Canepari,¹ G. Capello,² R. B. Ijaduola,² A. Cuneo,² L. Ying,²
F. Fratnik,² A. Colavita²

¹Laboratory of Biophysics & INFM Unit, International School for Advanced Studies, Trieste, Italy

²Microprocessor Laboratory ICTP/INFN, Trieste, Italy

Summary This paper presents technical details, hardware and software of a complete imaging system which uses a fast CCD sensor and a 41 Msample/s A/D converter to acquire full-frame 12 bit/pixel digitised images with a time resolution of 1.25 ms/image. This apparatus permits to resolve intracellular Ca^{2+} , gradients in individual cells as well as the spatio-temporal pattern of neural activity of cell assemblies in neural tissue.

INTRODUCTION

Optical methods are interesting to physiologists and neuroscientists for several reasons [1]. Of particular importance is the capability of recording simultaneously from multiple sites and the possibility of reaching fast sampling rates. Therefore, it is fundamental to develop imaging systems that, combining both features, achieve a high spatio-temporal resolution. In this respect, CCD sensors are well suited for detecting low-light level signals from fluorescent probes introduced into living cells [2]. These devices possess high quantum efficiency for converting light into electrical signals that allow monitoring variations in the intracellular concentration of Ca^{2+} and other fundamental ions within the cell cytoplasm. This paper provides a detailed description of an imaging system based on a sensitive CCD sensor with high readout rate (15 MHz). Sensor's output was digitised at 12 bit/pixel by customised electronics permitting image acquisition rates of up to 735 frames/s with a full-frame resolution of 128×128 pixels. The noise characteristics and the photon

the system were analysed in detail. The system's capability to visualise dynamic Ca^{2+} fluorescence, both from individual cells and from cell assemblies, was tested using different cell preparations and experimental protocols. Gradients of intracellular Ca^{2+} concentration were detected in outer hair cells of the guinea-pig cochlea and pyramidal neurones of the rat hippocampus by individually loading cells embedded in their native tissue with the impermeant form of Calcium Green-1 or Oregon Green-1. Propagation of Ca^{2+} bursts in the CA3 and CA1 regions of the hippocampus, associated to epileptogenic activity produced by direct stimulation of CA3 pyramidal neurones following blockade of GABA-mediated inhibition with bicuculline, was monitored in slices previously incubated with the membrane permeable form of fluo-3. The high spatio-temporal resolution achieved by this apparatus can be of value in investigating the time-course of rapid Ca^{2+} fluorescence transients, such as those associated with neuronal action potentials near physiological temperature.

MATERIALS AND METHODS

Construction of the system

Figure 1 presents a block-diagram of the recording system that was built around an upright microscope, mounted on a vibration isolation table, and included a CCD detector unit, a digital frame-grabber and a PC. A

Received 20 July 1998

Revised 27 October 1998

Accepted 28 October 1998

Correspondence to: Dr Fabio Mammano, Laboratory of Biophysics & INFM Unit,
International School for Advanced Studies, via Beirut 2-4, 34014 Trieste, Italy
Tel.: +39 (040) 3787 254; fax: +39 (040) 3787 249; e-mail: mammano@sissa.it

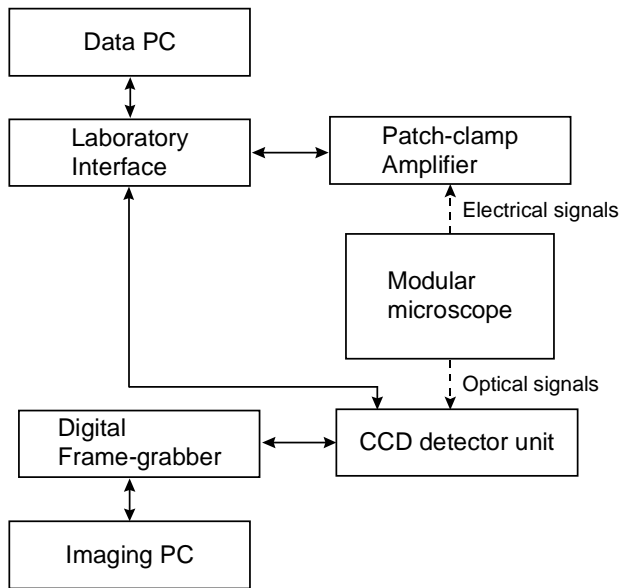


Fig. 1 Schematics of the recording system.

second PC was used to drive a laboratory interface for the synchronisation of optical and electrical signals from the cell preparation placed on the microscope stage.

CCD detector unit

The core of the optical recording section was a fast CCD sensor with 128×128 pixels (DALSA IA-D1). The sensor was attached to a copper plate thermo-electrically cooled by a 50 W Peltier device (Marlow Industries Inc.) driven by a variable power supply. The CCD output was digitised at 12 bit/pixel using a specialised A/D conversion circuit, whose block diagram is shown in Figure 2. The circuit consisted of surface-mount electronic devices (SMD) placed on a 6-layer printed circuit board (PCB) containing separate layers that were routed using low-noise arrangement techniques. Low-noise FET-input operational amplifiers (OPA655, Burr Brown) having large band width, low distortion and low bias current were selected for this design.

The board's input was amplified in voltage by the inverting buffer and sent to the correlated double sampling (CDS) section whose function was to reduce the detrimental effects of low frequency noise (low relatively to the pixel frequency) and slow power supply and temperature drifts. This was achieved by taking the pixel-by pixel difference between CCD internal reference (porch) and pixel level (Fig. 2B). The underlying assumption is that porch and pixel values are equally affected by low frequency noise, coherent over a time-scale comparable to the clock period. For each period of the CCD clock, a capacitor in the CDS circuit is charged to the porch voltage during phase (a). The switch is opened during

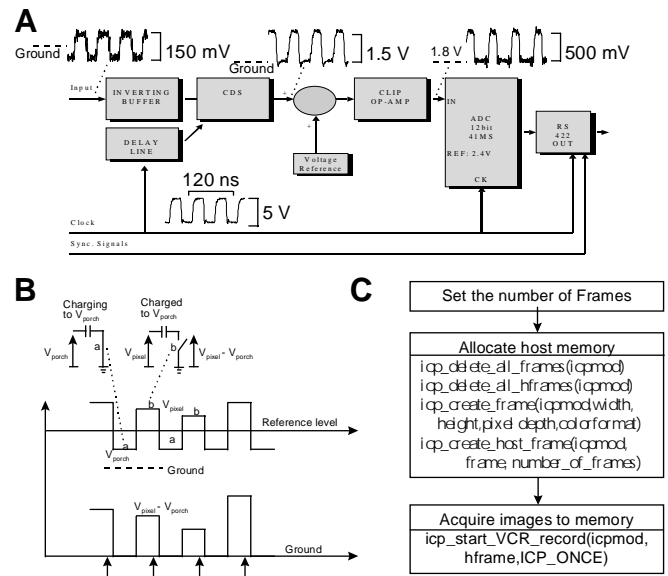


Fig. 2 (A) Block diagram of the 12 bit A/D image digitisation board. Typical waveforms, sampled at 1 GHz using a digital oscilloscope (LC574A, LeCroy) from the crucial points of the circuits, are reproduced for clarity. The CCD output video signal is formed by an alternation of internal reference (porch) and pixel voltage: each pixel signal in an image is separated from the next one by the porch voltage. Pixel frequency is under control from an external clock and can be increased up to 15 MHz. (B) Idealised waveforms to show how the CDS circuit measures the difference between porch and pixel value at each tick of the CCD clock. *Top*: CDS input. *Bottom*: output. (C) Software flow-chart, using the image-acquisition library (*ITEX-IC Core*) supplied by the manufacturer of the frame grabber. First the number of frames to be acquired was specified. Then host memory was allocated using host memory allocation functions. Finally, all frames in a sequence were acquired with a single call to the high-level function *icp_start-VCR record*.

the successive phase (b) allowing the difference between pixel and porch voltage to be measured by the A/D converter at the times marked by vertical arrows. The lower limit of the capacitor's value was determined by the desire to achieve a settling time shorter than the shortest clock semi-period (about 30 ns), taking into account the finite output impedance of the operational amplifiers. The upper bound was set by the constraint that the capacitor should not discharge appreciably (i.e. less than 1 part in 4096) through the parasitic resistance during one semi-period. A compromise value was found to be 50 pF. Output from the CDS entered a summing block where the black-level reference was displaced by adding a reference voltage and the result was sent to the clip op-amp. This was used to increase the dynamic range of the A/D converter by the removal of the signal fraction below the black-level reference and to protect the converter's sensitive input from out-of-range signals. The A/D converter adopted for this design (AD9042, Analog Devices) performed nominal 12 bit conversions at a maximum rate of 41 million samples/s. Digital output was

converted to standard RS422 differential signal by a set of line drivers (AM26C31, Texas Instruments).

Acquisition and storage of optical signals

The CCD detector unit operated in frame-transfer mode, with photo-charge integration time amounting to 96% of the inter-frame interval. During the remaining 4%, pixel data were shifted from the light-exposed to the masked region of the CCD. Digitised pixel values were output from the 12 pairs of RS422 differential lines and fed to a 16 bit digital frame grabber (IC-PCI/AM-DIG16, Imaging Technology) controlled by dedicated software. The software permitted the sequential capture of frames at the maximum rate compatible with the sensor's electronics (735 frames/s) without frame loss and up to the capacity of the PC's RAM. In a typical experiment, sequences of 100-1000 frames were stored in RAM and saved off-line on a UW SCSI hard drive either as raw binary data or as Audio Video Interlaced files (AVI, Microsoft Video for Windows RIFF format). Computer programs used to drive the frame grabber were written in Visual C++ using object-level real-time library code (ITEX-IC Core) supplied by the manufacturer and were executed on a 133 MHz Pentium PC operating under Windows 95 (Fig. 2C). The control signals required to trigger image acquisition were generated by a 12-bit laboratory interface (1401 plus, Cambridge Electronic Design) using customised control software running on a second PC (see Fig. 1). The frame-valid (FVAL) pulses, produced by the CCD sensor whenever a frame-transfer operation was completed, were sampled by the same interface in order to trace image timing.

Fluorescence imaging

The microscope (MI 250, Newport-Microcontrole) was equipped with infinity-corrected water-immersion objectives (x10, N.A. 0.30; x20, N.A. 0.50; x40, N.A. 0.75; x63, N.A. 0.90; Achroplan, Carl Zeiss) and a custom made epifluorescence illuminator incorporating an excitation interference filter and a long-pass dichroic mirror (D480/30x and 505DCLP, Chroma Technology Corporation). Excitation light from a 75-W stabilised Xenon arc source (CAIRN Research Ltd.) was coupled to the microscope via a liquid light guide gated by a rapid shutter (UniBlitz, Vincent Associates). Fluorescence emission was selected using a second pair of dichroic blade and interference filter (XF23, Omega Optical). This filter set was optimised for the calcium-selective dye Calcium Green-1.

Fluorescence images were formed on the fast CCD sensor using an achromatic doublet as projection lens (Fig. 3). Distances in the image plane were calibrated by placing a 10 μm pitch graticule under the objective.

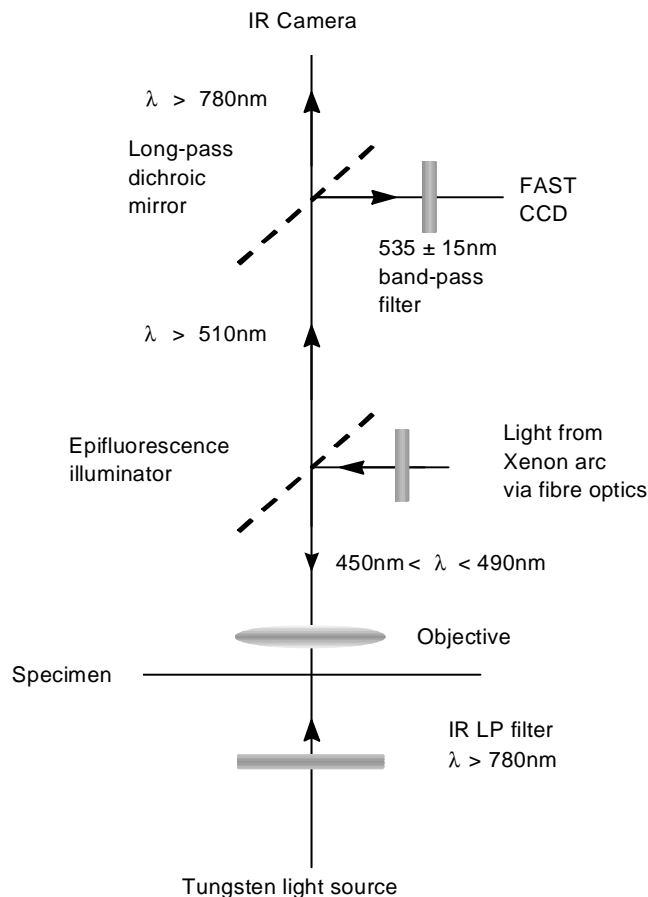


Fig. 3 Scheme of the optics.

A second projection lens was used to form IR images of the specimen on a conventional CCD camera operating at standard video rate with the spatial resolution allowed by the PAL signal (768 \times 576 pixels). The entire optical group was mounted on a system of X-Y-Z motorised translators that allowed it to be moved with respect to the imaged sample. For each image pixel, fluorescence signals were computed as ratios:

$$\Delta F(t)/F(0) = [F(t) - F(0)]/F(0)$$

where t is time, $F(t)$ is fluorescence following a stimulus that causes calcium elevation within the cell and $F(0)$ is pre-stimulus fluorescence computed by averaging 10-20 images. Both $F(t)$ and $F(0)$ were corrected for mean autofluorescence computed from a 20 \times 20 pixel rectangle devoid of obvious cellular structures. Ratio magnitude was encoded by 8 bit pseudo-colour look-up tables to produce false-colour images. This local ratio computation is expected to provide correction for time-independent non-uniformity in optical path-length and dye concentration [3]. Light was attenuated with a diaphragm to avoid phototoxicity by reducing

to $\leq 0.5\%/s$. Images were analysed using routines developed from Matlab 5.1 Image Processing Toolbox (The Mathworks Inc.). Where reported, images were smoothed with a 3x3 two-dimensional median filter [4] and fluorescence traces were smoothed with a three-point zero-phase digital filter [5].

Cell preparation and electrophysiological recordings

In order to test the suitability of the system for biological fluorescence imaging, two different preparations were used: (1) intact organ of Corti from the isolated guinea pig cochlea [6] and (2) hippocampal slices from rat brain [7]. Although very different in nature, both preparations preserved the cellular organisation of their native tissue, while simultaneously allowing optical and electrical recording from single identified cells. Whole-cell patchclamp recordings [8] were made using an EPC/7 amplifier (List Medical, Darmstadt, Germany) to drive pipettes pulled on a two-stage vertical puller (PP-83, Narishige) from 1.5 mm o.d. soda glass (Clark Electromedical). Pipettes were filled with the cell impermeant forms of the Ca^{2+} -selective fluorescent dyes Calcium Green-1 (75 μM ; C-3010, Molecular Probes) or Oregon Green-1 (100 μM ; 0-6806, Molecular Probes) dissolved in a solution containing (in mM): 123 K-gluconate, 12 KCl, 4 MgCl_2 , 10 HEPES, 0.3 Na_2GTP , 10 Phosphocreatine and 50 units/ml of Creatine Phosphokinase, adjusted to pH 7.2 with KOH and brought to 300-325 mOsm/litre with D-glucose [7]. The pipette resistance was typically 3 M Ω when measured in the bath. The organ of Corti was continuously superfused at 2 ml/min with an artificial perilymph solution containing (in mM): NaCl, 142; KCl, 4.0; CaCl_2 , 1.0; MgCl_2 , 2.0; Na_2HPO_4 , 8.0; NaH_2PO_4 , 2.0, adjusted to pH 7.3 with NaOH and osmolality 325 ± 2 mOsm/L with D-glucose. Hippocampal slices of 200 μm thickness were superfused at the same rate with a solution containing (in mM): 126 NaCl, 3.5 KCl, 2 CaCl_2 , 1.2 NaH_2PO_4 , 1.3 MgCl_2 , 25 NaHCO_3 , 11 glucose, bubbled with 95% O_2 and 5% CO_2 . For some experiments, 20 μM of the dye fluo-3 (membrane permeable acetoxymethyl (AM) ester form; F-1241, Molecular probes) was added to the medium and slices were pre-incubated for 1-2 h at 32 $^\circ\text{C}$. For pressure application of drugs, a puff pipette, prepared similarly to the patch pipette, was placed 50-100 μm above the cell and pressure was applied at its back by a Pneumatic PicoPump (PV800, World Precision Instruments) gated by a TTL pulse under software control. Larger pipettes (10-20 μm) were used to convey monopolar extracellular electrical stimuli to the tissue from an isolated stimulator (A385, World

Precision Instruments). Except where specified, experiments were performed at room temperature and drugs were purchased from SIGMA.

RESULTS AND DISCUSSION

Validation of the system

Acquisition performance

To assess the capability of the recording system to acquire high-speed sequences of frames, a LED digital counter was built and clocked by FVAL pulses, each FVAL pulse incrementing the counter by one digital unit. The framegrabber driver allowed the user to allocate up to 2^{32} bytes of physical RAM (not virtual memory). It follows that, in principle, the maximum amount of PC memory that could be reserved for acquisition was limited only by the available RAM, although in the present configuration only RAM sizes up to 128 Mbytes were tested. Careful analysis of images generated by focusing the sensor onto the counter (Fig. 4A) revealed that frame storage to PC RAM and subsequent dump to the hard drive occurred with no frame loss for up to 3500 consecutive images (each stored image occupied 32 Kbytes and the operating system required some 10 Mbytes to run efficiently).

Linearity

Linearity was checked by illuminating a sample of 10 μm diameter fluorescent beads (FluoSperes; F-8830, Molecular Probes) placed on a microscope cover slip under the objective (Fig. 4B). A sequence of 100 images was acquired at the rate of 735 frames/s and bead fluorescence was measured from several points of the view field and plotted vs. illumination intensity level (Fig. 4C). Illumination was varied by changing the aperture of the diaphragm in front of the fibre optics and its intensity was measured with a photodiode placed on the illumination light path after the dichroic blade. The input/output function was linear over a wide range of intensities and irrespective of the position of the sample in the view field, indicating that the system was well suited for dynamic fluorescence measurements.

Noise figure

The overall noise associated with the acquisition of an image by a CCD device is:

$$N_T = (N_R^2 + N_D^2 + N_{ph}^2)^{1/2}$$

where N_R and N_D are the readout noise and the dark-charge noise of the CCD, respectively, and N_{ph} is the photon shot-noise associated with the fluorescence signal. The sensor's full-well capacitance was about 3.8×10^5 e $^-$. When it was illuminated to half-saturation under constant and uniform conditions, without cooling, the single-pixel noise, measured during sequence acquisition

¹When recording from brain slices, the intracellular solution contained also 4.0 mM ATP.

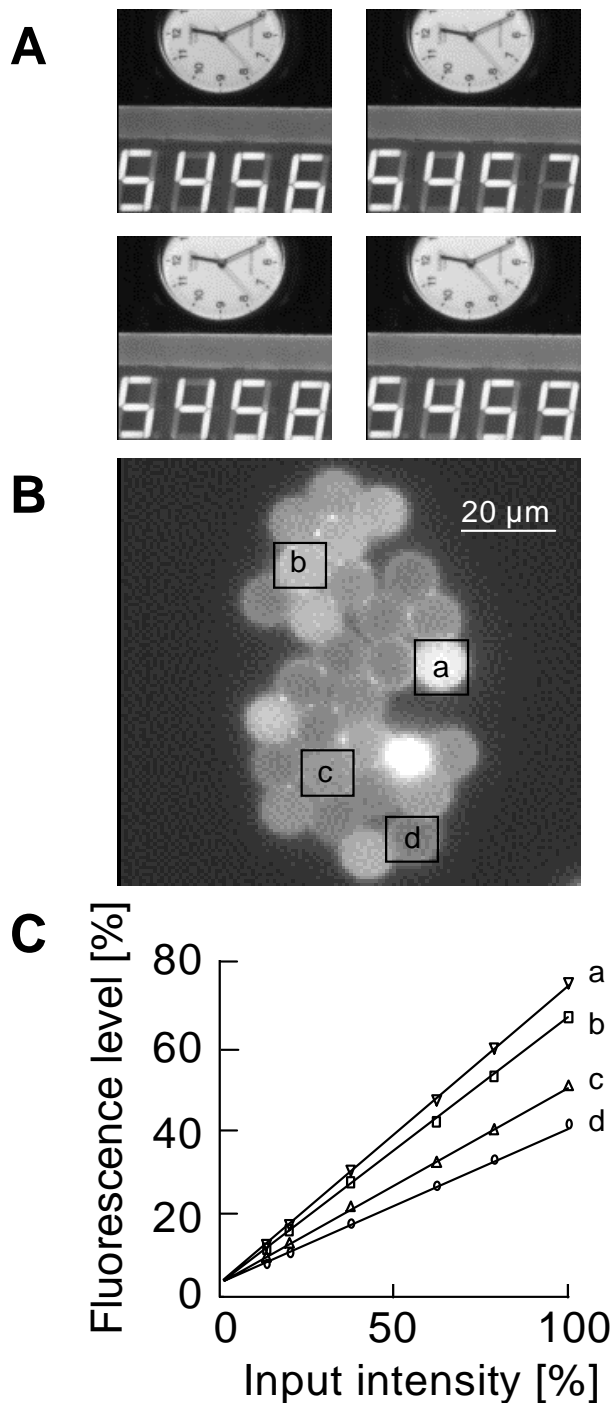


Fig. 4 System validation. (A) Consecutive digital images of a LED counter clocked by the FVAL signal of the CCD. Images show no lag in response, indicating that the effective speed of the optical recording system is that of the FVAL signal (max. 735 frames/s). (B) Image of fluorescence beads clustered on a microscope coverslip. Fluorescence intensity was measured from the four regions of interest (ROIs), labelled (a) to (d), for a set of 100 frames acquired at 735 frames/s. (C) Bead fluorescence, averaged within each ROI and over the whole 100 frame sequence, is plotted against normalised illumination intensity for the four ROIs shown in (B). Solid lines are linear least-square fits to data. Error bars are smaller than plot symbols and are not shown. Extrapolation to zero input gives non-zero output because of residual offset, affecting the CCD signal prior to digitisation.

© Harcourt Brace & Co. Ltd 1999

acquisition at the maximum frame rate, was approximately 2.5 bits. As N_{ph} is the square root of the photoelectron number, the contribution to the overall noise from the electronics was of the order of ~ 300 e $^-$. This figure, which at 735 frames/s is due almost exclusively to N_R , can be assumed as an upper bound for the electronics noise at all frame rates. In fact, N_R decreased whereas N_D increased when reducing the speed of acquisition, but N_D was kept efficiently under control by cooling the sensor. The contribution from N_D to the total noise was negligible for frame rates of ≥ 200 frames/s, even without cooling, and was rendered negligible for frame rates down to 50 frames/s by keeping the sensor at 15°C. Maximum background fluorescence intensities $F(0)$ of the order of 4×10^4 photoelectrons/ms/pixel were consistently achieved by loading cells with Calcium Green-1 or Oregon Green-1 at concentrations of 75–100 µM, while using illumination levels that did not cause either photodamage or appreciable bleaching over repeated exposure periods of 100–200 ms. Therefore, the minimum $\Delta F(t)/F(0)$ signal detectable with a $S/N \cong 1$, was of the order of 1% at the minimum inter-frame interval of 1.36 ms. In practice, from experiments conducted on living cells within brain slices, we determined that 1.5 ms should be taken as the shortest viable inter-frame interval for biological fluorescence imaging applications. The S/N could be increased by a factor ~ 2.5 by operating the sensor in 2×2 binning mode, i.e. by collecting four times as many photons per pixel at the same rate (the frame rate can be doubled in binning mode, if desired, and memory requirements are obviously reduced to 1/4 under these conditions).

Intracellular Ca^{2+} gradients in sensory cells

Outer hair cells (OHCs) from the mammalian cochlea (Fig. 5A) were selected for this first set of experiments. Their characteristic elongated shape and cylindrical symmetry makes OHCs particularly suitable for demonstrating the system's capability to reveal differential distributions of Ca^{2+} elevation in the cytoplasm. Individual OHCs were patch-clamped in situ as previously described [6] and filled with 75 \sim µM Calcium Green-1 through the patch electrode. Following dye equilibration (10–15 min), cells were held at potentials of from -60 to -50 mV and exposed for 1–2 s to focal pressure application of adenosine 5'-triphosphate (ATP, 100 µM; A-5394, SIGMA). In isolated OHCs, ATP is known to activate an inward current partly owing to Ca^{2+} influx [9], and to produce elevation of intracellular Ca^{2+} level [10, 11] by the activation of P2 purinergic receptors located on the cell stereocilia [12]. In the isolated cochlea, ATP directed onto the stereocilia of OHCs elicited inward cationic currents (Fig. 5B, top) that were associated with rapid increases of

Cell Calcium (1999)25(2), 115–123

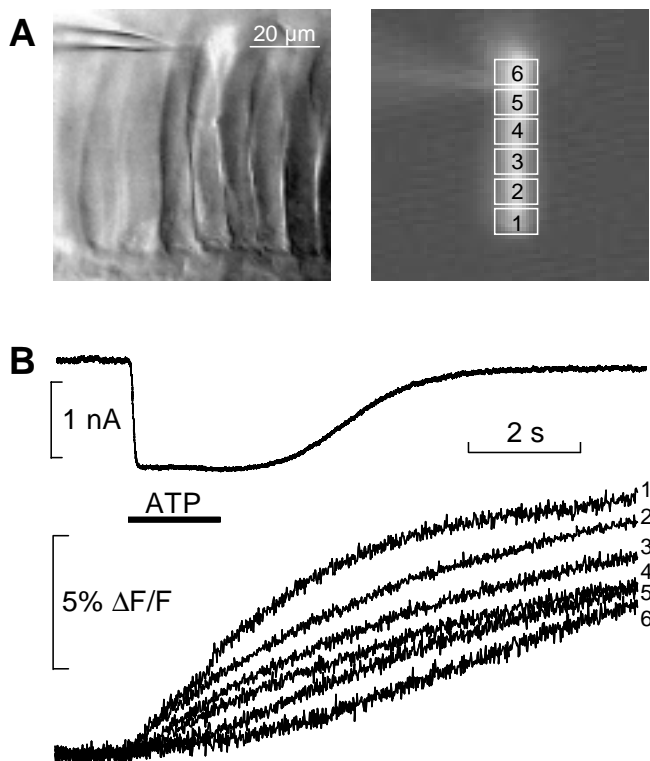


Fig.5 Outer hair cell response to extracellular ATP. (A) Left: IR image of outer hair cells within turn two of the organ of Corti, seen from scala media in an isolated cochlea preparation. Stereocilia are visible near frame bottom. A patch pipette entering from left, is contacting one outer hair cell. Right: fluorescence image of the patched cell, taken from a sequence of 980 frames. A set of six regions of interest (ROIs) is shown superimposed. (B) Top: inward current elicited by pressure application of ATP (1100 μ M) from a pipette held about 50 μ m above the stereocilia. Bottom: time-course of Ca^{2+} fluorescence changes measured from the ROIs in (A). Inter-frame interval

rapid increases of calcium fluorescence (Fig. 5B, bottom). The increase of Ca^{2+} concentration was initially localised near the stereocilia and propagated to the rest of cytoplasm on a time scale of seconds, indicating the development of a substantial concentration gradient along the cell axis. Ca^{2+} levels remained elevated for several minutes, long after the inward current had ceased, and gradually returned to baseline, presumably as a consequence of cell buffering and extrusion. Further applications of ATP were generally unable to produce responses of amplitude comparable to the first, causing instead an irreversible increase of the resting leakage current, probably owing to the opening of Ca^{2+} -activated non-selective cation channels [13].

Ca^{2+} entry following action potentials in neurones

Detection of optical signals at a temporal resolution of the order of milliseconds is required in many interesting physiological applications. An important example is the

recording of Ca^{2+} signals following firing activity in neurones, known to trigger a broad spectrum of intra- and inter-cellular responses [14]. Ca^{2+} entry evoked by trains of action potentials has been monitored in pyramidal neurones of the hippocampus [15] and cortex [16] using cooled CCD devices operating at a maximum rate of 100 frames/s. We visualised Ca^{2+} fluorescence by dye-loading individual CA3 and CA1 pyramidal neurones in hippocampal brain slices while simultaneously measuring cell potential using the patch-clamp technique. The maximum firing frequency in hippocampal neurones is known to be limited by the rapid inactivation of A-type K^{+} channels [17,18]. This phenomenon is strongly temperature-dependent, the maximum firing frequency being an increasing function of temperature. At physiological temperature pyramidal neurones can fire up to almost 100 Hz; therefore, acquiring images at 100 frames/s was insufficient to reveal the contribution to Ca^{2+} entry from individual action potentials in a train (Fig. 6A, green traces). Lowering the interframe-interval to below 2 ms permitted to resolve the finer details of both temporal (Fig. 6A, red traces) and spatial evolution of Ca^{2+} transients (Fig. 6B). We verified that image acquisition at rates of >200 frames/s is unnecessary at normal room temperature (22–24°C), as the time-course of Ca^{2+} fluorescence is limited by the relaxation time of the dye- Ca^{2+} binding reaction (approximately 5 ms; data not

Spatio-temporal patterns of neural activity in brain slices

One application of optical recording techniques is the study of nervous activity originating from different locations of neuronal networks. Fluorescence imaging has been applied to the detection of electrical signals from simple invertebrate networks [20,21] as well as from networks in the central nervous system (CNS) of mammals [22,23]. The dynamics of neuronal circuits can be analysed by monitoring Ca^{2+} fluorescence simultaneously from several neurones [24]. Figure 7 shows two sequences of images from CA3 (left) and CA1 (right) regions of the rat hippocampus in a slice pre-incubated with the AM-ester form of fluo-3 (see Materials and Methods). Extracellular electrical stimulation of the stratum radiatum near the dentate gyrus, in the presence of 10 μ M bicuculline to remove inhibition from GABA-ergic interneurones, induced burst discharges that originated in the CA3 region and propagated to the CA1 [25]. The CA3 image sequence clearly shows Ca^{2+} entry in two identified pyramidal neurones. Signal propagation within the slice could be easily followed, at room temperature, by capturing images at the rate of 100 frames/s. The high spatio-temporal resolution analysis of signal propagation

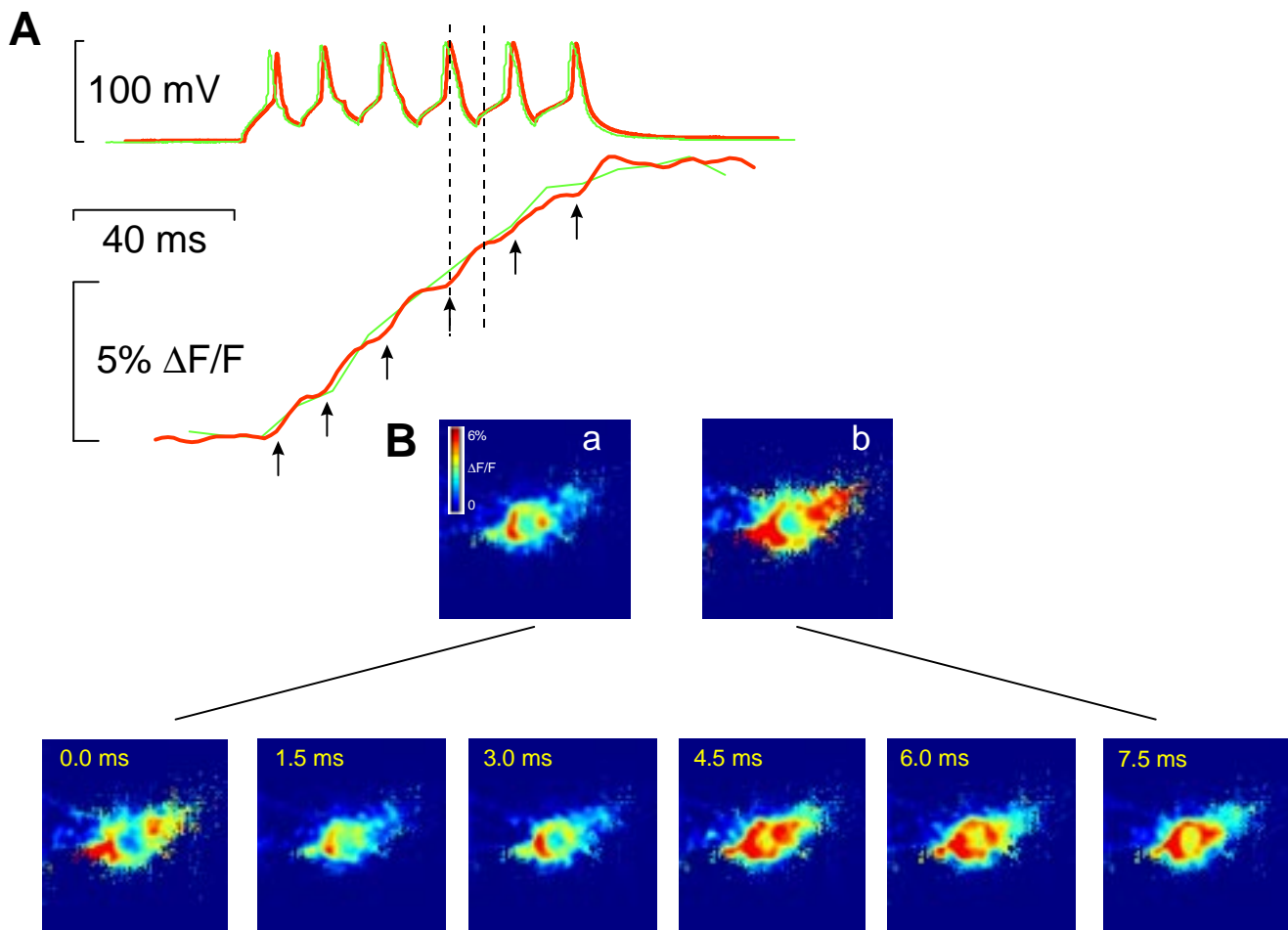


Fig. 6 Neuronal response to repeated somatic current injection at near-physiological temperature. (A) Top, left: cell potential measured in current-clamp mode from a CA3 pyramidal neurone within a hippocampal brain slice. Current pulses of 150 pA were delivered at 66 Hz repetition frequency, eliciting trains of action potentials from a resting potential of -70 mV. The mean inter-spike interval during the trains was 15 ms. Green and red traces correspond to two successive acquisitions from the same cell. Bottom, left: Ca^{2+} fluorescence time courses averaged from the square region drawn in the neurone image on the right and measured simultaneously to the trains of action potentials. Green and red traces correspond to image sequences captured at 119 and 658 frames/s respectively (red trace smoothed with a three-point zero-phase digital filter). Vertical arrows correspond to the peaks of action potentials. The cell was loaded with 100 μM Oregon Green 1 through the patch pipette. (B) Top: pair of consecutive false-colour images collected at 119 frames/s at the times marked by vertical cursors a and b (green traces in A). Bottom: six consecutive images collected over the same time span at 658 frames/s (red traces in A). Experiment performed at 32 °C.

of the mammalian CNS, such as the hippocampus [26], can contribute significantly to the understanding of complex brain functions.

CONCLUSIONS

The purpose of this paper was to illustrate the performance of an optical recording system developed for fast biological imaging. It was constructed by assembling a range of different optical and electronic components and optimised for high-speed detection of fluorescence emissions from long-wavelength Ca^{2+} -selective probes. At the core of the optical detection section we placed a low-cost commercial CCD sensor, originally designed for industrial applications, whose output was digitised by a specialized

developed for this project. This allowed image capture at rates of up to 735 frames/s, with the possibility of acquiring over 3500 full-frame images in sequence with 12 bit/pixel accuracy. Such high rates and sensitivity result from the good quantum efficiency of the sensor (40%) and the extremely high speed at which frames were transferred from the unmasked to masked regions of the CCD. As the overhead for frame transfer time was reduced to a mere 4% of the interframe interval, photo-charge integration was particularly efficient. The recording apparatus was tested by monitoring the dynamics of intracellular Ca^{2+} in experiments conducted on cells within highly organized sensory and neural tissues. The results demonstrated its versatility and potentiality, especially in cases in which high rates of acquisition were required.

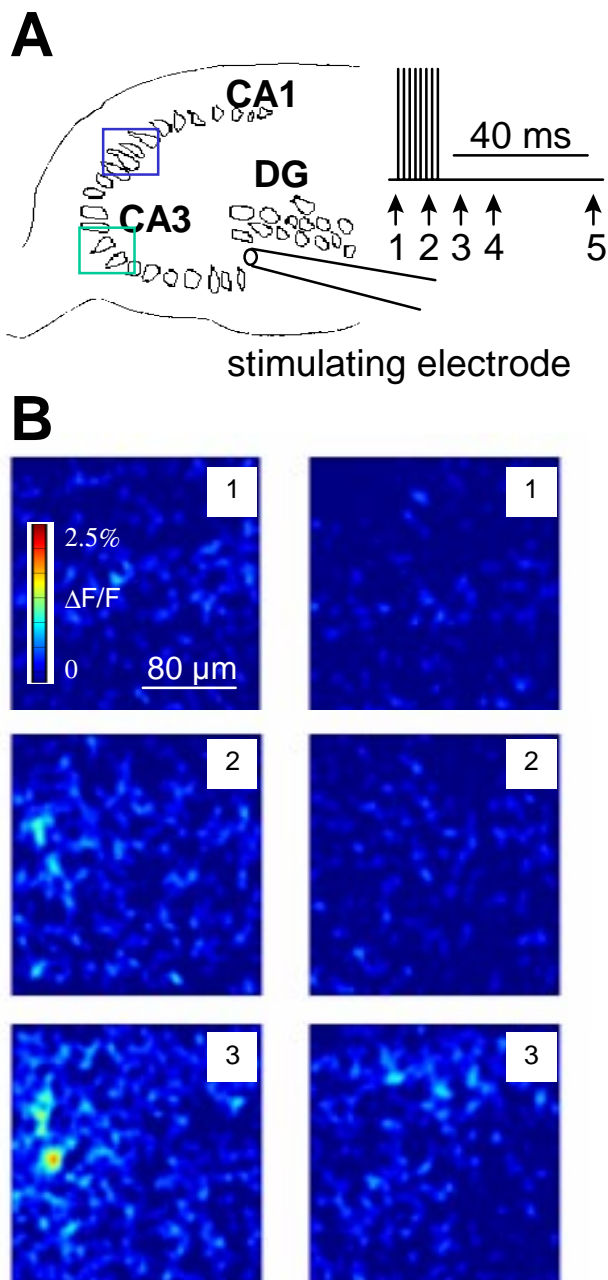


Fig. 7 Calcium signal propagation in a neuronal network. (A) Schematic drawing of a hippocampal slice from an 11-day-old rat, pre-incubated for 2 h at 32°C with a solution containing 20 μM fluo3 AM-ester and subsequently superfused in standard slice solution (see Materials and Methods) to which 10 μM bicuculline was added. The extracellular stimulating electrode was positioned near the dentate gyrus (DG) region. Calcium fluorescence was imaged in two distinct compartments, one in the CA3 region (green box) and one in the CA1 region (blue box). Timing of stimulation and frame capture is shown as inset. Trains of eight pulses at 50 Hz were delivered while images were collected at 10 ms inter-frame interval. (B) Two sets of five selected false-colour images from the sequences acquired during different stimulation periods while imaging the areas indicated in (A). The colour scale-bar is reproduced on the first image. The number on each image correspond to the timing indicated in (A). The colour of the numbers correspond to the colour of the contoured regions in (A). Images were smoothed with a 3x3 two-dimensional median filter.

acquisition were required. CCD-based cameras previously described and utilised for applications in the field of biological imaging achieved rates in the order of 100 frames/s only at the expense of spatial resolution. As demonstrated by the experiment in Figure 6, this relatively high frame rate is still not sufficient to reveal the details of fast events such as the rapidly evolving intracellular Ca^{2+} concentration gradients following neuronal firing at physiological temperature.

In principle, the system described here can be made to operate also in ratiometric mode using fura-2 in combination with a fast-switching wave-length selector (e.g. Polychrome II; TILL Photonics) with an expected maximum rate of 329 frame-pairs/s, although this was not tested. The major drawbacks of this design is the lack of confocality. However, this may not necessarily constitute a serious limitation for several interesting experimental situations where 2D-signal propagation patterns, like those illustrated in Figures 6 and 7, are the main focus. In this respect, it is worth mentioning that, if the investigated sample possess near-radial symmetry, the optical sectioning power of the fluorescence microscope can be improved substantially by restricting the illumination field [27].

ACKNOWLEDGEMENTS

Supported by SISSA Grant N.2101 'Nuove Iniziative di Sviluppo', by INFM grant PRA-CADY and by the United Nations University (Tokio, Japan). We thank Professor Enrico Cherubini for critical comments on the ms.

REFERENCES

1. Cohen L. Special topic: Optical approaches to neural function. *Ann Rev Physiol* 1989; **51**: 487-490.
2. Lasser-Ross N, Miyakawa H, Lev-Ram W, Young SR, Ross WN. High time resolution fluorescence imaging with a CCD camera. *J Neurosci Meth* 1991; **36**: 253-261.
3. Neher E, Augustine GJ. Calcium gradients and buffers in bovine chromaffin cells. *J Physiol* 1992; **450**: 273-301.
4. Lim JS. Two Dimensional Signal and Image Processing. Prentice Hall, Englewood Cliffs 1990; NJ. 469-476.
5. Oppenheim AV, Shaffer RW. Discrete-Time Signal Processing. Prentice Hall, Englewood, Cliffs 1989; NJ. 311-312.
6. Mammiano F, Kros CJ, Ashmore JF. Patch clamped responses from outer hair cells in the intact adult organ of Corti. *Pflügers Archiv* 1995; **430**: 745-750.
7. Canepari M, Cherubini E. Dynamics of excitatory transmitter release: analysis of synaptic responses in CA3 hippocampal neurones after repetitive stimulation of afferent fibres. *J Neurophysiol* 1998; **79**: 1977-1988.
8. Hamill O, Marty A, Neher E, Sakmann B, Sigworth FJ. Improved patch-clamp techniques for high resolution current recording from cells and cell-free membrane patches. *Pflügers Archiv* 1981; **391**: 85-100.
9. Nakagawa T, Akaike N, Kimitsuki T, Komune S, Arima T. ATP-induced current in isolated outer hair cells of the guinea-pig cochlea. *J Neurophysiol* 1990; **63**: 1068-1074.

10. Ashmore JF, Ohmori H. Control of intracellular calcium by ATP in isolated outer hair cells of the guinea-pig cochlea. *J Physiol* 1990; **428**: 109-131.
11. Ashmore JF, Kolston PJ, Mammano F. Dissecting the outer hair cell feedback loop. In: Duifhuis H (ed.) *Biophysics of Hair Cell Sensory Systems*. Singapore, World Scientific, 1993; 151-158.
12. Mockett BG, Housley GD, Thorne PR. Fluorescence imaging of extracellular purinergic receptor sites on isolated cochlear hair cells. *J Neurosci* 1994; **14**: 6992-7007.
13. Abbeele Van Den T, Tran Ba Huy P, Teulon J. Modulation by purines of calcium-activated non-selective cation channels in the outer hair cells of the guinea-pig cochlea. *J Physiol* 1996; **494**: 77-89.
14. Ghosh A, Greenberg ME. Calcium signaling in neurons: Molecular mechanisms and cellular consequences. *Science* 1995; **268**: 239-247.
15. Callaway JC, Ross WN. Frequency-dependent propagation of sodium action potentials in dendrites of hippocampal CA1 pyramidal neurons. *J Neurophysiol* 1995; **74**: 1395-1403.
16. Helmchen F, Imoto K, Sakmann B. Ca^{2+} buffering and action potential-evoked Ca^{2+} signaling in dendrites of pyramidal neurons. *Biophys. J* 1996; **70**: 1069-1081.
17. Kopysova IL, Debanne D. Critical role of axonal A-type A-Type K^+ channels and axonal geometry in the action potential propagation along CA3 pyramidal cell axons: a simulation study. *J Neurosci* 1998; **18**: 7436-7451.
18. Martina M, Schultz JH, Ehmke H, Monyer H, Jonas P. Functional and molecular differences between voltage-gated K^+ channels of fast-spiking interneurons and pyramidal neurons of rat hippocampus. *J Neurosci* 1998; **18**: 8111-8125.
19. Kao JP, Tsien RY. Ca^{2+} binding kinetics of fura-2 and azo-1 from temperature-jump relaxation measurement. *Biophysical J* 1988; **53**: 635-639.
20. Wu JY, Cohen LB, Falk CX. Neuronal activity during different behaviours in aplysia: a distributed organisation. *Science* 1994; **263**: 820-823.
21. Canepari M, Campani M, Spadavecchia L, Torre V. CCD imaging of electrical activity in the leech nervous system. *Eur Biophys J* 1996; **24**: 359-370.
22. Delaney KR, Gelperin A, Fee MS, Flore JA, Gervais R, Tank DW, Kleinfeld D. Waves and stimulus modulated dynamics in an oscillating olfactory network. *Proc Natl Acad Sci USA* 1994; **91**: 669-673.
23. Obaid AL, Salzberg BM. Simultaneous optical-recording of electrical-activity with single cell resolution from several ganglia in a mammalian plexus. *J Gen Physiol* 1996; **107**: 353-368.
24. Garaschuk O, Hanse E, Konnerth A. Developmental profile and synaptic origin of early network oscillations in the CA1 region of rat neonatal hippocampus. *J Physiol* 1988; **507**: 219-236.
25. Wong RKS, Traub RD. Synchronised burst discharge in disinhibited hippocampal slices I. Initiation in the CA2-CA3 region. *J Neurophysiol* 1983; **49**: 442-458.
26. Iijima T, Witter MP, Ichikawa M, Tominaga T, Kajiwara R, Matsumoto G. Entorhinal-hippocampal interactions revealed by real-time imaging. *Science* 1996; **272**: 1176-1179.
27. Hiraoka Y, Sedat JW, Agard DA. Determination of three-dimensional imaging properties of a light microscope system. *Biophysical J* 1990; **57**: 325-333.